Communication

Demonstration of Molecular Assembly on Si (100) for CMOS-Compatible Molecule-Based Electronic Devices

Nadine Gergel-Hackett, Christopher D. Zangmeister, Christina A. Hacker, Lee. J. Richter, and Curt. A. Richter

J. Am. Chem. Soc., **2008**, 130 (13), 4259-4261 • DOI: 10.1021/ja800378b

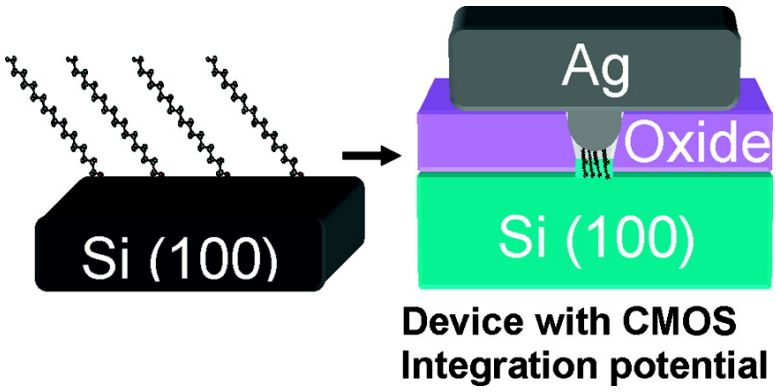

More About This Article

Additional resources and features associated with this article are available within the HTML version:

- Supporting Information
- Links to the 1 articles that cite this article, as of the time of this article download
- Access to high resolution figures
- Links to articles and content related to this article
- Copyright permission to reproduce figures and/or text from this article

View the Full Text HTML

J|A|C|S
COMMUNICATIONS

Published on Web 03/07/2008

Demonstration of Molecular Assembly on Si (100) for CMOS-Compatible Molecule-Based Electronic Devices

Nadine Gergel-Hackett,*,† Christopher D. Zangmeister,‡ Christina A. Hacker,† Lee. J. Richter,‡ and Curt. A. Richter†

Semiconductor Electronics Division, Electronics and Electrical Engineering Laboratory, and Chemical Science and Technology Laboratory, National Institute of Standards and Technology, Gaithersburg, Maryland 20899

Received January 16, 2008; E-mail: nadinegh@nist.gov

In this work, we show that organic monolayers can be assembled on Si (100) that are comparable in quality, aliphatic monolayer coverage, and extent of substrate oxidation to those assembled on the more extensively studied Si (111) crystal face. These monolayers enable the successful fabrication of molecular electronic devices on Si (100) substrates that exhibit molecule-dependent electrical characteristics and have the potential for integration with traditional silicon-based technologies. The use of 100-oriented Si is imperative for increasing the compatibility of molecular electronic devices with existing CMOS technologies; however, the majority of self-assembly on Si for use in molecular electronic devices has been performed on substrates with (111) crystalline orientation (motivated, in part, by the nearly ideal surfaces achieved by H termination in buffered HF).[1−7] While there has been limited investigation of solution-phase monolayer assembly on the hydrogen passivated Si (100) crystal face,[8−11] the device fabrication and electrical characterization of monolayers on Si (100) performed to date have relied on nonmetallic "soft" device top contact materials (such as mercury drops, carbon nanotubes, or electrolytes).[12−14] These "soft" contacts have been used to avoid displacement or degradation of the monolayer during the metal evaporation;[15,16] however, the use of these materials limits the molecular devices to be integrated with existing Si technologies and circuits. One of the main obstacles to realizing a hybrid molecular/Si technology is the prevalent use of CMOS-incompatible materials in molecular electronic devices and test structures.[17−27] By assembling monolayers on the CMOS-compatible Si (100) and circumventing the need for "soft" top contacts through the use of evaporated silver (which does not displace directly attached molecules),[15] we fabricated devices with increased future integration potential that show molecule-dependent electrical characteristics.

Monolayers of aliphatic alcohols and thiols were assembled by using a UV-assisted procedure previously developed for molecular assembly on Si (111).[1] The quality of the monolayers on both heavily and lightly doped Si (100) was compared to identically prepared films on Si (111) with spectroscopic ellipsometry (SE), X-ray photoemission spectroscopy (XPS), and Fourier transform infrared spectroscopy (FTIR). The SE-determined thickness for each sample is shown on the left-hand axis of Figure 1a and ranged between 1.6 and 2.4 nm. (The theoretical calculated molecular length is ∼2.4 nm.) Full XPS scans from 1100 to 0 eV that were obtained for each sample contained only Si, C, S, and O, the elements of the monolayer and substrate, indicating molecular purity. Also shown in Figure 1a is the ratio of the monolayer C 1s peak intensity to the substrate Si 2p peak intensity, corrected for sensitivity factors. The trends in the SE and XPS agree well, and both indicate that there is no observed overall difference in quality

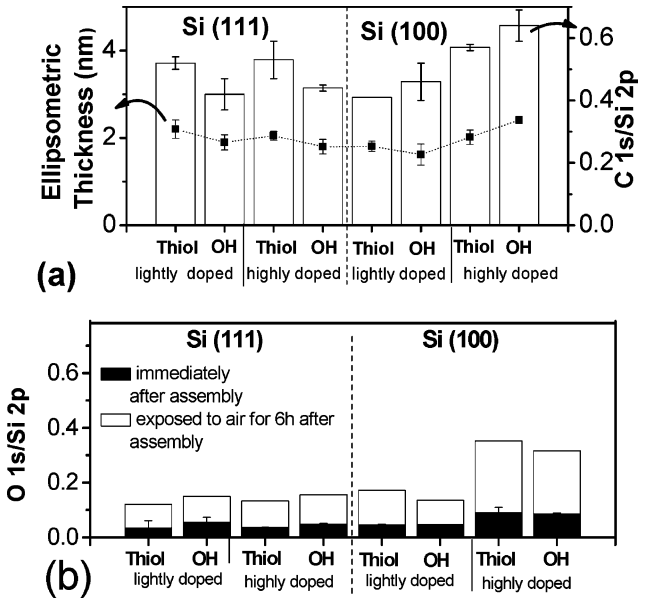

Figure 1. (a) XPS peak intensity ratio of C 1s/ Si 2p (right-side, open bars) and ellipsometric thickness (left-side, solid squares) of thiol and alcohol terminated monolayers on lightly and highly doped Si (100) and Si (111) substrates. (b) O 1s/Si 2p XPS peak ratios for thiol and alcohol monolayers assembled on lightly and highly doped Si (111) and Si (100) substrates immediately after monolayer assembly and after the monolayers were exposed to the ambient for 6 h.

or coverage between those monolayers assembled on Si (100) and those assembled on Si (111). The intensity of the CH stretching bands in the FTIR of the samples shows similar trends (see Supporting Information).

The differences between the samples with different functional groups, wafer orientations, and substrates fall within the range of uncertainty for the various characterization methods when data from SE, XPS, and FTIR are included. By using four different methods to estimate surface coverage from these data (see Supporting Information for description of methods) and averaging the results, we were able to estimate a surface coverage for each of the samples of approximately $3 \pm 1 \times 10^{14}$ cm^{-2}. This density is consistent with FTIR spectroscopy of the CH_2 asymmetric stretch that indicates moderate gauche disorder in the alkane chains compared to highly crystalline films, such as octadecanetrichlorosilane (OTS) monolayers assembled on silicon dioxide.[28] Chain conformational order is a subtle function of packing density. The areal densities of liquid and solid alkanes differ by only about 10%. The difference in areal densities is estimated by using the density of a densely packed crystal of paraffin (an ordered long-chain alkane solid) of 0.93 g/cm^3 and the density of liquid dodecanethiols of 0.845 g/mL.

† Electronics and Electrical Engineering Laboratory.
‡ Chemical Science and Technology Laboratory.

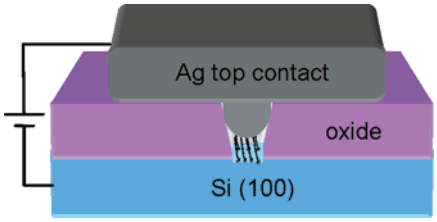

Figure 2. Cross section of the molecular electronic device structure.

The monolayer quality can be further inferred by its ability to block the growth of silicon oxide. XPS was used to characterize the extent of the substrate oxidation that occurred after monolayer formation. The O 1s/Si 2p XPS peak ratios for the lightly and heavily doped Si (100) and Si (111) samples immediately after removal from an oxygen-free environment and after 6 h of air exposure are shown in Figure 1b. Making the assumption that all of the measured oxygen is contained at the silicon surface and attenuated by the molecular overlayer, we used this XPS data to calculate the surface O/Si ratios for the samples.[3] From the O 1s/Si 2p XPS peak ratios of 0.03−0.35 shown in Figure 1b, we calculated that the ratios of oxygen to silicon atoms on the substrate surface ranged from 0.7 to 1.7 for the freshly prepared samples and from 2.0 to 5.9 for those exposed to air for 6 h (one SiO_2 monolayer is expected to have a O to Si ratio of approximately 2, assuming that all the O 1s signal emanates at the Si-molecule interface). The calculated ratios for the unexposed films are in the range of those previously reported for similar self-assembled monolayers on Si (111) and indicate that the oxide layer formed on the surface prior to long-term air exposure is less than a monolayer.[3] This lack of significant oxidation of the surface is supported by the negligible SiO_2 features in the FTIR spectra. The lack of a full monolayer of oxide also reinforces that the observed SE thickness accurately represents the thickness of the aliphatic monolayer (Figure 1a).

There is no clear correlation evident between the order of the film (as determined via FTIR) or the density of the film (as determined via SE and XPS) and the oxidation of the monolayer over time. There was no evidence for the oxidation of the adsorbed thiol, based on the position of the S 2s peak (226 eV, see Supporting Information). The S 2s peak was used to determine the extent of the thiol oxidation, instead of the S 2p peak that is traditionally used for molecules assembled on metals, because Si has a 2s peak at 155 eV that overlaps with the S 2p peak, making shifts in S 2p position difficult to detect for monolayers on Si.

To directly assess the monolayers assembled on Si (100) for potential use in technological applications, we fabricated enclosed planar molecular electronic devices with alkanethiols. Alkanethiols have been widely studied for use in molecular electronic devices, and because their expected mode of electron transport is simple quantum mechanical tunneling, they are expected to exhibit a current vs molecular chainlength dependence.[13,29] By fabricating and comparing Si (100)-based devices containing alkanethiols of at least two different chainlengths, we confirmed the effectiveness of the assembly technique on Si (100) for use in molecular electronic devices.

The basic device structure (schematically shown in cross section in Figure 2) begins with a hydrogen-terminated silicon bottom of a 5 μm × 5 μm well through a thermally grown oxide layer. Monolayers (octadecanethiol or dodecanethiol) were then assembled on the bottom silicon, and the device was capped with a thermally evaporated top Ag contact. This structure is one of a few that are fabricated with the molecular monolayer encapsulated in an oxide

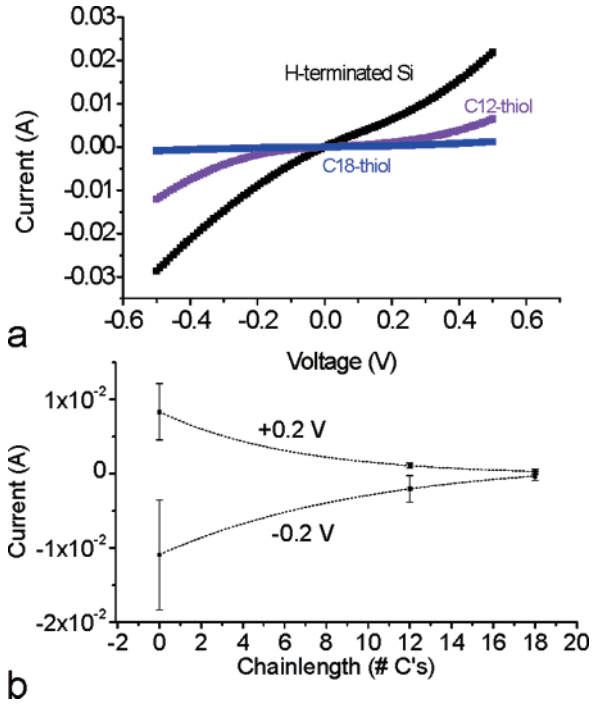

Figure 3. (a) Representative I−V curves for two different chainlengths of molecules assembled on Si (100) and the hydrogen terminated silicon control. (b) Chainlength vs median current at +0.2 and −0.2 V for multiple devices.

well capped with metal, rather than having multiple metal top contacts directly deposited onto a single monolayer assembled over a large area.[15,30−32] The control devices consisted of the hydrogen-terminated silicon/Ag junction with no monolayer assembled. Ag was used as the top contact material for all of the devices because it has been observed not to displace the molecules in the junctions during top contact evaporation.[15] Degenerately doped silicon was used to increase the likelihood that the electrical behavior of the device was dominated by the quantum mechanical tunneling through the molecular monolayer, rather than being dominated by the surface depletion field due to the Schottky barrier between the silicon and the silver top contact.[32] The resistance of the silicon substrate contact was tested and was found to be negligible relative to the resistance of the device junction. The complete details of the fabrication are given in the Supporting Information.

Figure 3a shows representative current−voltage (I−V) curves for the Si (100)-based molecular electronic devices. Figure 3b shows the current-chainlength dependence of the devices at 0.2 and −0.2 V. Each data point of Figure 3b represents the median current magnitude of a different chainlength molecular device. The median current values and standard deviations represented include data from all of the devices tested that exhibited a current magnitude within 4 times the median current for the devices with the same molecular chainlength. In total, 21 devices from multiple experimental runs were tested. Of these devices, 18 showed current magnitudes that were within 4 times the median current, resulting in an overall "working" device yield of 86%.

From these data, it is evident that the electrical characteristics of the devices are inversely dependent on the presence/absence of molecules and the molecular chainlength, which indicates that the electrical behavior of the devices is molecule-dependent.[13,29] However, the degree of the dependence is not as strong as would be expected based on classic tunneling models through a rectangular insulating barrier with the same thickness as that of the molecular film.

One possible explanation for the weaker current vs chainlength dependence could be changes in the film structure with alkane chain length. In earlier studies of alcohol attachment to Si (111), optimal film order, as judged by FTIR, was achieved for shorter (~C13) chains.[1] The relative film densities of the C18-thiol and C12-thiol monolayers can be deduced from their SE thicknesses by taking into account their relative chainlengths. This interpretation of the SE as an indication of aliphatic coverage is valid due to the lack of oxide in monolayers as determined via FTIR and XPS. The SE film thickness for the C12-thiol monolayer was approximately 1.5 nm, which, taking into account the relative chainlengths of C18-thiol (2.4 nm) and C12-thiol (1.6 nm), indicates that the C18-thiol assembled on the degenerately doped Si is less dense than the C12-thiol. Thus, there is the possibility that some of the observed chain length dependence is due to structural changes. However, the variation of current with ellipsometric thickness (vs carbon number) still deviates strongly from expectations based on simple tunneling.

Other factors that may contribute to the observed decreased dependence of current on molecular chainlength when compared to classic tunneling models include the effects of: contact image charges, molecular polarization of the film, mixing of the silicon electronic states with the molecular electronic states,[29] and/or a silicon surface depletion field tunneling barrier that results from the work function mismatch between the Ag and the silicon.[13,29] Other work with metal-molecule-Si devices has also exhibited current/chainlength trends that are different than would be expected for classical tunneling through a rectangular barrier.[13,29] A quantitative analysis of the device characteristics is beyond this report. Such a study, including the influence of strongly electron withdrawing molecular films, is underway. Overall, the molecular dependence observed for these Si (100) devices illustrates the potential for direct assembly to be used to fabricate technologically relevant molecule-dependent electronic devices.

Acknowledgment. This work was funded in part by the NIST Office of Microelectronics Programs and the DARPA MoleApps Program. The research was performed while NGH held a National Research Council Research Associate Award at the National Institute of Standards and Technology.

Supporting Information Available: A description of experimental methods, Fourier transform infrared spectroscopy of the aliphatic monolayers, X-ray photoelectron spectroscopy of the monolayers, a description of the methods used for estimating the coverage of the aliphatic monolayers. This information is available free of charge via the Internet at http://pubs.acs.org.

References

(1) Hacker, C. A.; Anderson, K. A.; Richter, L. J.; Richter, C. A. *Langmuir* **2005**, *21*, 882−889.
(2) Boukherroub, R.; Morin, S.; Sharpe, P.; Wayner, D. D. M.; Allongue, P. *Langmuir* **2000**, *16*, 7429−7434.
(3) Cicero, R. L.; Linford, M. R.; Chidsey, C. E. D. *Langmuir* **2000**, *16*(13), 5688−5695.
(4) Eves, B. J.; Sun, Q.-Y.; Lopinski, G. P.; Zuilhof, H. *J. Am. Chem. Soc.* **2004**, *126*(44), 14318−14319.
(5) Zharnikov, M.; Kuller, A.; Shapoenko, A.; Schmidt, E.; Eck, W. *Langmuir* **2003**, *19*, 4682−4687.
(6) Barrelet, C. J.; Robinson, D. B.; Cheng, J.; Hunt, T. P.; Quate, C. F.; Chidsey. C. E. D. *Langmuir* **2001**, *17*, 3460−3465.
(7) de Villeneuve, C. H.; Pinson, J.; Bernard, M. C.; Allongue, P. *J. Phys. Chem. B* **1997**, *101*(14), 2415−2420.
(8) Balakumar, A.; Lysenko, A. B.; Carcel, C.; Malinovski, V. L.; Gryko, D. T.; Schweikart, K. H.; Loewe, R. S.; Yasseri, A. A.; Liu, Z.; Bocian, D. F.; Lindsey, J. S. *J. Org. Chem.* **2004**, *69*(5), 1435−1443.
(9) Sun, Q. Y.; de Smet, L. C. P. M.; van Lagen, B.; Giesbers, M.; Thune, P. C.; van Engelenburg; de Wolf, F. A.; Zuilhof, H.; Sudholter, E. J. R. *J. Am. Chem. Soc.* **2005**, *127*, 2514−2523.
(10) De Smet, L. C. P. M.; Pukin, A. V.; Sun, Q. Y.; Eves, B. J.; Lopinski, P.; Visser, G. M.; Zuilhof, H.; Sudholter, E. J. R. *Appl. Surf. Sci.* **2005**, *252*, 24−30.
(11) Guisinger, N. P.; Greene, M. E.; Basu, R. U.; Baluch, A. S.; Hersam, M. C. *Nano Lett.* **2004**, *4*, 55.
(12) Roth, K. M.; Yasseri, A. A.; Liu, Z.; Dabke, R. B.; Malinovski, V.; Schweikart, K. H.; Yu, L.; Tiznado, H.; Zaera, F.; Lindsey, J. S.; Kuhr, W. G.; Bocian, D. F. *J. Am. Chem. Soc.* **2002**, *125*, 505−517.
(13) Faber, E. J.; De Smet, L. C. P. M.; Olthius, W.; Zuilhof, H.; Sudholter, E. J. R.; Bergveld, P.; Van de Berg, A. *Chem. Phys. Chem* **2005**, *6*, 2153−2166.
(14) He, J.; Chen, B.; Flatt, A. K.; Stephenson, L. J.; Coyle, C. D.; Tour, J. M. *Nat. Mater.* **2006**, *5*, 63−68.
(15) Hacker, C. A.; Richter, C. A.; Gergel-Hackett, N.; Richter, L. J. *J. Phys. Chem. C* **2007**, *111*(26), 9384−9392.
(16) Fisher, G. L.; Walker, A. V.; Hooper, A. E.; Tighe, T. B.; Bahnck, K. B.; Skriba, H. J.; Reinard, M. D.; Haynie, B. C.; Opila, R. L.; Winograd, N.; Allara, D. L. *J. Am. Chem. Soc* **2002**, *124*, 5528−5541.
(17) Zhou, C.; Deshpande, M. R.; Reed, M. A.; Jones, L., II; Tour, J. M. *Appl. Phys. Lett.* **1997**, *71*, 611.
(18) Reed, A. M.; Chen, L.; Rawlett, M. A.; Price, W. D.; Tour, M. J. *Appl. Phys. Lett.* **2001**, *78*, 3735.
(19) Fan, F. F.; Yang, J.; Cai, L.; Price, D. W.; Dirk, S. M.; Kosynkin, D. V.; Yao, Y.; Rawtlett, A. M.; Tour, J. M.; Bard, A. J. *J. Am. Chem. Soc.* **2002**, *124*, 5550.
(20) Donhauser, Z. J.; Mantooth, B. A.; Kelly, K. F.; Bumm, L. A.; Monnell, J. D.; Stapleton, J. J.; Price, D. W., Jr.; Rawlett, A. M.; Allara, D. L.; Tour, J. M.; Weiss, P. S. *Science* **2001**, *292*, 2303.
(21) Chen, J.; Reed, M. A.; Rawlett, A. M.; Tour, J. M. *Science* **1990**, *286*, 1550.
(22) Wold, D. J.; Frisbie, C. D. *J. Am. Chem. Soc.* **2001**, *123*, 5549.
(23) Bumm, L. A.; Arnold, J. J.; Cygan, M. T.; Dunbar, T. D.; Burgin, T. P.; Jones, L., II; Allara, D. L.; Tour, J. M.; Weiss, P. S. *Science* **1996**, *271*, 1705.
(24) Cui, X. D.; Zarate, X.; Tomfohr, J.; Sankey, O. F.; Primak, A.; Moore, A. L.; Moore, T. A.; Gust, D.; Harris, G.; Lindsay, S. M. *Nanotechnology* **2002**, *13*, 5.
(25) Amlani, I.; Rawlett, A. M.; Nagahara, L. A.; Tsui, R. K. *Appl. Phys. Lett.* **2002**, *80*, 2761.
(26) Kushmerick, J. G.; Holt, D. B.; Yang, J. C.; Naciri, J.; Moore, M. H.; Shashidhar, R. *Phys. Rev. Lett.* **2002**, *89*, 086802.
(27) Gergel-Hackett, N.; Majumdar, N.; Martin, Z.; Swami, N.; Pattanaik, G.; Zangari, G.; Zhu, Y.; Pu, L.; Yao, Y.; Tour, J. M.; Harriott, L. R.; Bean, J. C. *J. Vac. Sci. Technol. A* **2006**, *24*(4), 1243.
(28) Richter, C. A.; Hacker, C. A.; Richter, L. J.; Kirillov, O. A.; Suehle, J. S.; Vogel, E. M. *Solid-State Electron.* **2006**, *50*, 1088−1096.
(29) Soloman, A.; Boecking, T.; Seitz, O.; Markus, T.; Amy, F.; Chan, C.; Zhao, W.; Cahen, D.; Kahn, A. *Adv. Mater.* **2007**, *19*, 445−450.
(30) Majumdar, N.; Gergel, N.; Routenberg, D.; Li, B.; Pu, L.; Yao, Y.; Tour, J. M.; Bean, J. C.; Harriott, L. R. *J. Vac. Sci. Technol. B* **2005**, *23*(4), 1417.
(31) Wang, W.; Lee, T.; Kamdar, M.; Reed, M. A.; Stewart, M. P.; Hwang, J. J.; Tour, J. M. *Superlattices* **2003**, *33*, 217−226.
(32) Scott, A.; Janes, D. B.; Risko, C.; Ratner, M. *Appl. Phys. Lett.* **2007**, *91*, 033508.

JA800378B